

5. ANNEXES – ADDITIONAL PAPERS

5.1. EVALUATION OF DOPPLER ULTRASONOGRAPHY FOR THE MEASUREMENT OF BLOOD FLOW IN YOUNG LOGGERHEAD SEA TURTLES (*CARETTA CARETTA*) (IN PRESS)



Valente, A.L.; Parga, M.L.; Espada, Y., Lavin, S.; Alegre, F.; Marco, I. and Cuenca, R. (2007). Evaluation of Doppler ultrasonography for the measurement of blood flow in young loggerhead sea turtles (*Caretta caretta*). Vet. J. Aceptado para publicación. Doi: 10.1016/j.rvj..2007.03.006

Available online at www.sciencedirect.com

The Veterinary Journal xxx (2007) xxx-xxx

The
Veterinary Journalwww.elsevier.com/locate/yvjl

Evaluation of Doppler ultrasonography for the measurement of blood flow in young loggerhead sea turtles (*Caretta caretta*)

Ana Luisa Valente^{a,*}, Maria Luz Parga^b, Yvonne Espada^c, Santiago Lavin^a,
Ferrán Alegre^b, Ignasi Marco^a, Rafaela Cuenca^a

^a *Servei d'Ecopatologia de Fauna Salvatge, Facultat de Veterinària, Universitat Autònoma de Barcelona, 08193 Bellaterra, Barcelona, Spain*

^b *Centre de Recuperació d'Animals Marins, Camí Real, 239, 08330 Premià de Mar, Barcelona, Spain*

^c *Departament de Medicina i Cirurgia Animal, Facultat de Veterinària, Universitat Autònoma de Barcelona, 08193 Bellaterra, Barcelona, Spain*

Accepted 9 March 2007

Abstract

The aim of this study was to identify ultrasound accessible blood vessels in the loggerhead sea turtle (*Caretta caretta*) and describe their Doppler waveform patterns, peak systolic velocity, mean velocity, systolic/diastolic ratio as well as pulsatility and resistive indices. B-mode, colour and pulsed-wave Doppler examinations were performed on 10 turtles. Flow measurements were recorded for the left and right aorta, epigastric and internal iliac arteries, and right hepatic vein. Additionally, the large blood vessels of three dead turtles were injected with latex and dissected for anatomical support. A parabolic flow velocity profile was observed in all arteries. The waveforms of the right and left aortic arteries showed an unusual pattern when compared with mammals. The hepatic vein flow velocity waveform of the loggerhead sea turtle was found to be similar to that in the dog, although the flow velocity in the C-wave was higher than that in the A-wave. The low resistance flow pattern observed suggests that the loggerhead sea turtle's organs require a continuous blood supply. © 2007 Published by Elsevier Ltd.

Keywords: Loggerhead sea turtle; Blood flow; Doppler wave patterns; Ultrasonography; Reptiles

Introduction

The loggerhead sea turtle (*Caretta caretta*) is an endangered species often admitted to marine rescue centres in the Mediterranean region. As is the case with other species of chelonians, health assessment poses a formidable challenge for reptilian veterinarians due to the animals' specific morphology and physiology (Murray, 2006a), and ancillary methods are usually required to obtain an accurate diagnosis. Turtles in a state of shock or with no external reaction to mechanical stimuli are frequently admitted to rehabilitation centres (Balazs, 1986; Stabenau et al., 2001). Loggerhead sea turtles captured in fishing nets usually display, on first appraisal, signs of drowning and/or shock (Balazs,

1986; Stabenau et al., 2001), and it is frequently difficult to distinguish between a live and a recently deceased turtle.

Doppler ultrasonography represents a non-invasive technique that is useful for the routine examination of blood flow in the vessels of many domestic species (Szatmári et al., 2001; Fernández del Palacio et al., 2003). It is an inexpensive technique suitable for repeated measurements and with a wide field of applications. In sea turtles, previous ultrasound studies have focused the reproductive physiology (Rostal et al., 1990) and the normal ultrasonographic B-mode appearance of cervical structures and coelomic organs (Valente et al., in press). Information concerning the use of Doppler ultrasound in sea turtles has not however been found in the literature. Accurate measurements of blood flow are essential in haemodynamic studies and could be useful in establishing a diagnosis in injured sea turtles, help in resuscitation procedures (Stabe-

* Corresponding author. Tel.: +34 93 581 19 23; fax: +34 93 581 20 06.
E-mail address: schifinoval@hotmail.com (A.L. Valente).

u et al., 2001) and to monitor anaesthetized patients (Murray, 2006b).

Reptiles have a complex cardiovascular system, quite different from that of mammals. They have many venous sinuses, ventricles incompletely subdivided into two chambers, aortic arteries and a renal portal system (Wyncken, 2001; Murray, 2006a; Holz, 2006). Data on cardiovascular physiology in chelonians are widely scattered in the literature and are characterized by significant gaps. To the authors' knowledge, a description of haemodynamic measurements for clinical application in sea turtles has not been published.

The purpose of this study was to identify blood vessels easily accessed by ultrasound in this species and describe their Doppler waveform patterns, peak systolic velocity, mean velocity, systolic/diastolic ratio and pulsatility (PI) and resistive (RI) indices. Gross anatomical information of the circulatory system (including the portal renal system) is provided to support the identification of the vessels examined.

Materials and methods

B-Mode, colour and pulsed-wave Doppler examinations were performed in 10 loggerhead sea turtles (four juveniles and six sub-adults), using an Acuson ultrasound machine (Computed Sonography Siemens XP/10), in conjunction with 5.0, 6.0 and 7.0 MHz sector phased array transducers. The turtles showed a minimum straight carapace length of 0–58.5 cm, a weight range of 3.5–26.8 kg, and were accidentally caught pelagic long-line sets and fishing nets along the North-western Mediterranean coast (40°31'–42°26'N and 0°32'–3°10'E) of Spain.

During the study the turtles were temporarily housed in the rehabilitation facilities of the Rescue Centre for Marine Animals (CRAM), Premià de Mar, Barcelona, Spain. Only turtles in good condition, based on physical, radiographic and haematological parameters, were used in this study.

The animals were manually restrained in ventral recumbency without anaesthesia. The Doppler evaluation was performed in a standard temperature-controlled room at an ambient temperature of 21–25 °C. Ultrasound examinations were performed in 10 acoustic windows (cervical-dorsal and cervical-ventral, left and right cervicobrachial, left and right axillary, left and right femoral and left and right postfemoral) (Valente et al., in press). Coupling gel (Polaris II, GE Medical Systems) was placed on the surface of the transducer, which was oriented mainly on the horizontal plane. B-mode imaging was used to examine the heart (seen in the cervical-ventral acoustic window) and large vessels and to guide the Doppler cursor placement in it. The same investigator performed all Doppler ultrasound examinations.

Following the orientation of the electronic callipers, Doppler tracings were recorded when an angle of 45° or less between the ultrasound beam and the direction of blood flow was achieved. Freeze trace and electronic cursors were used to make the measurements. The flow parameters resistive index (RI) and pulsatility index (PI) from each waveform specimen were measured and calculated using the internal callipers and the analytic software of the ultrasound unit following the formulae: $RI = (S - D)/S$; $PI = (S - D)/A$ and S/D ratio (systolic/diastolic), where S is the systolic peak (max velocity), D is the minimum diastolic velocity and A is the temporal mean velocity over one cardiac cycle (mean velocity). Schematic drawings indicating the acoustic windows and the vessels measured are shown in Fig. 1. Three dead turtles were injected with latex through the jugular vein, left and right aortic arteries and femoral vein. The large heart vessels and renal vasculature were dissected for additional morphological data. Specific anatomical terminology for sea turtles was adopted (Wyncken, 2001).

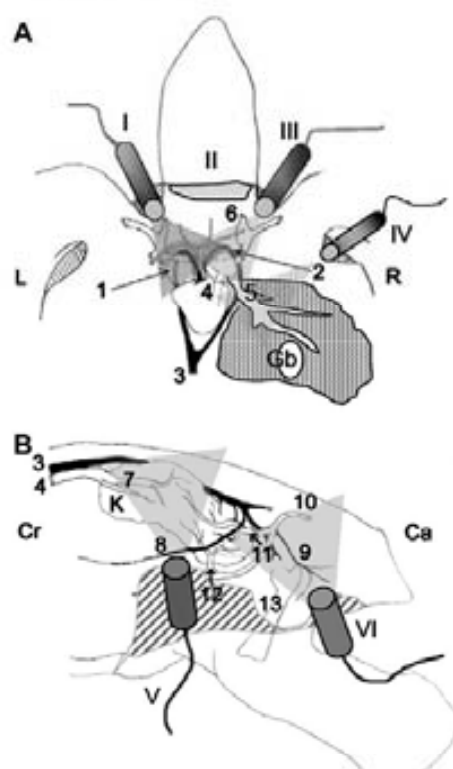


Fig. 1. Schematic drawings of the large vessels in the cardiac, hepatic and renal areas (some seen in the ultrasound examination) of loggerhead sea turtles. Arteries are represented in black and veins in white. (A) dorsal view of the area of the heart and (B) lateral view of the renal area: 1, left aorta; 2, right aorta; 3, abdominal aorta; 4, caudal vena cava; 5, right hepatic vein, Gb, gallbladder; 6, venous sinus at junction between jugular and brachial veins; 7, renal vein; 8, epigastric artery; 9, internal iliac artery; 10, iliac vein; 11, hypogastric vein (caudal portal renal vein); 12, epigastric vein (lateral portal renal vein); 13, femur. k, kidney; I, left cervicobrachial acoustic window; II, cervical-ventral acoustic window; III, right cervicobrachial acoustic window; IV, right axillary acoustic window; V, left prefemoral acoustic window; VI, left postfemoral acoustic window.

The data were analyzed statistically with STATISTICA for Windows (Stat Soft, Inc.) software. The data were tested for normality with the Shapiro–Wilk test. Paired t tests were used to compare flow measurements in paired vessels (left and right side) and differences were considered to be significant at $P < 0.05$.

Results

The mean heart rate was 29.1 beat/min (range 23–36). The highest rates (30–36 beat/min) were found in the juvenile turtles whereas values ranged between 23 and 32 beat/min in the sub-adults. Two sub-adult turtles with heart rates of 30 and 32 beat/min, respectively, were above the mean value for this group. In the juvenile turtles, the heart was entirely seen using a dorsal scan through the ventral cervical acoustic windows. An echocardiographic appearance of hyperkinetic ventricular motion with an exagger-

ated ventricular wall movement was observed. The left and right aortic arteries, epigastric and internal iliac arteries, and right hepatic vein were identified via ultrasonography but the iliac veins could not be visualised. The 7.0 MHz transducer was better for visualising the renal area and the postfemoral acoustic window. To assess the heart, aortic arteries and the right hepatic vein the 5.0 and 6.0 MHz transducers were used.

The left and right aortic arteries could be seen through the left and right cervicobrachial acoustic windows, respectively. From these windows, a complex image crossing many vessels was frequently observed at the cardiac base. Identification of the aortic arteries was based on their position, shape (a pronounced arch), large diameter (0.8–14.8 mm) and caudal blood flow direction (Fig. 2A and C). The vessel walls appeared as parallel, hyperechoic, thin lines. A cross-section of the left and right aortic arches was also seen when the cervical-dorsal window was examined. They were medial to the venous sinus formed by the junction of the external and internal jugular veins and the axillary vein on each side (Fig. 2B). However, in this acoustic window, the angle between the ultrasound beam and the vessels was in most cases almost perpendicular, generating unsuitable images for blood flow measurements. The visualisation of the aortic arteries through the ventral cervical acoustic window was inconsistent.

The waveforms of the right and left aortic arteries were similar. A parabolic flow profile without a spectral window was observed in eight turtles (Fig. 3A) and a discrete (mild) spectral window was present only in two turtles. Values of flow measurements and indices are showed in Table 1. No statistical differences were found between the flow parameters from the left and right aortic arteries. Compared with other arteries measured in this study, the aortic arteries showed the highest pulsatility and resistive indices.

The right hepatic vein and its junction with the caudal vena cava were clearly seen through the right axillary acoustic window, its echogenic wall enabling clear identification in the hepatic parenchyma. Close by, and positioned medially, the venous sinus of the right atrium was seen, and used as a landmark. Flow coming toward the transducer (above the baseline) and a triphasic pattern in the blood flow velocity profile was observed with A and C waves being identified. The C wave was higher than the A-wave (Fig. 3B).

Positioning the probe parallel to the carapace at the prefemoral acoustic windows enabled us to assess the left and right epigastric arteries, which crossed caudal to the kidneys and their gross anatomy indicated that they were not involved in blood supply to this organ (Fig. 4A). A parabolic flow velocity profile was observed (Fig. 3C; Table 1).

Anatomical dissections showed that most of the renal blood supply was provided by the renal portal system comprising two large renal afferent portal veins: the hypogastric vein, penetrating the kidney caudally, and the epigastric vein that enters this organ laterally in its cranial half (Fig. 5B). These veins and the renal arteries could not be

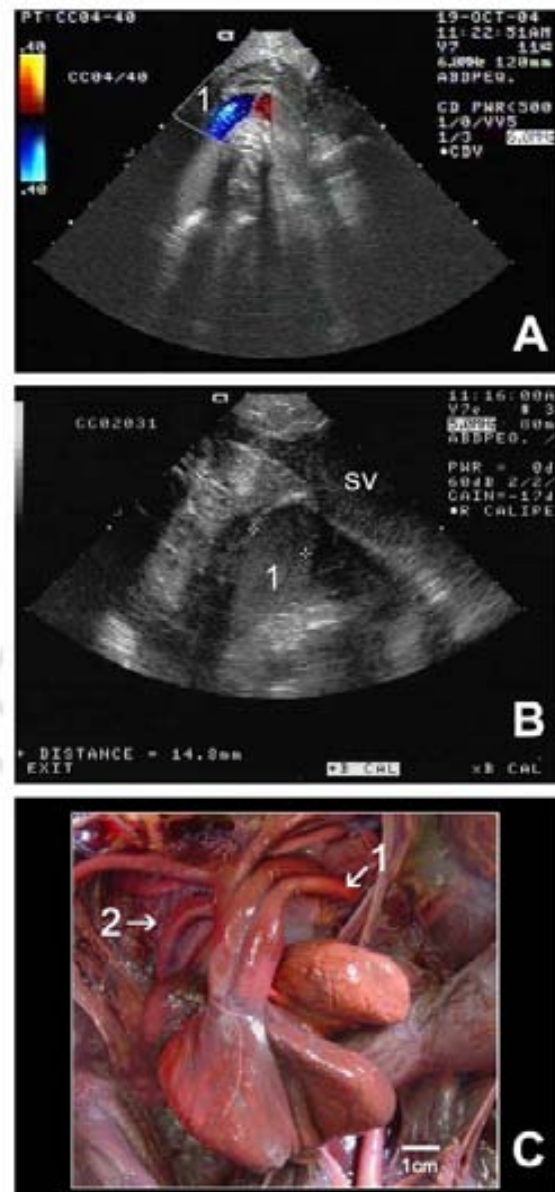


Fig. 2. (A) B-mode and colour flow Doppler ultrasound image of large vessels of loggerhead sea turtles seen through the left cervicobrachial acoustic window (red for Doppler shifts towards the ultrasound beam and blue for shifts away from it). (B) B-mode ultrasound image of the same arch seen through dorsal cervical acoustic window. Cursors measure the diameter. (C) Ventral view of dissected heart: 1, left aortic arch; 2, right arch (or right aortic arch); sv, sinus venous. (For interpretation of the references to colour in this figure legend, the reader is referred to the web version of this article.)

clearly identified in the ultrasound examination. Only the renal vein (a single large efferent renal vein as shown in Fig. 5A) could be observed consistently in the ultrasound

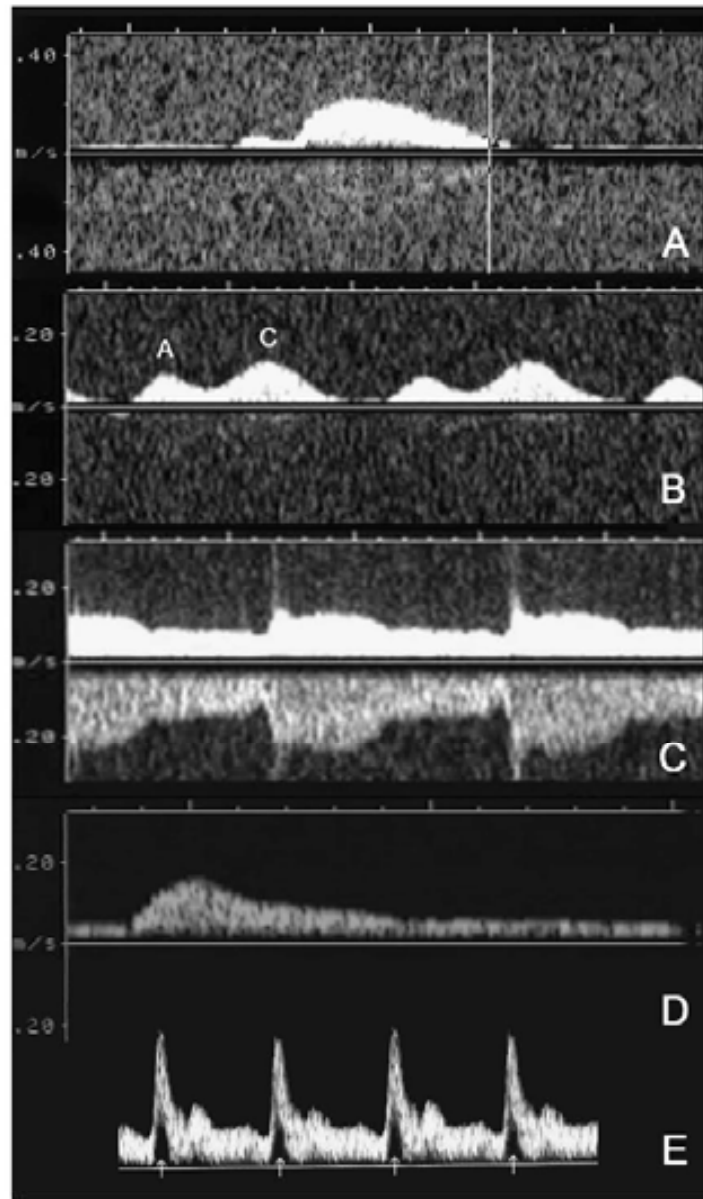


Fig. 3. Doppler waveforms of large vessels of loggerhead sea turtles. (A) aorta, (B) right hepatic vein (A and C-waves are indicated), (C) epigastric artery, (D) internal iliac artery and (E) normal pattern profile of the aorta of a mammal (arrows on the baseline indicate spectral windows).

examination, and was positioned cranial to the kidney (Fig. 4B and C).

The internal iliac arteries were identified in the postfemoral acoustic windows. The ultrasound beam was directed cranio-dorsally, dorsal to the hip joint. The arteries were consistently seen in the pelvic musculature passing dorso-caudally to the ilium (Fig. 6) and showed an unpronounced systolic peak followed by decreased continuous flow. Blood flow measurements are presented in Table 1.

Discussion

In humans and domestic animals it is known that endothelial dysfunction is present in individuals with arteriosclerosis and other causes of chronic heart failure, which could be diagnosed by abnormal responses in blood flow (Glagov et al., 1988; Kagawa et al., 1998). In the case of reptilians, there is scant information for clinicians concerning functional anatomy, circulatory physiology and pathology

Table 1

Peak systolic velocity (V_{max}), mean velocity (V_{mean}), pulsatility (PI) and resistive (RI) indices, and systolic/diastolic ratio in juvenile and sub-adult loggerhead sea turtles

Arteries	V_{max} (m/s)	V_{mean} (m/s)	PI	RI	Systole/diastole
Left aorta	0.22 ± 0.08	0.12 ± 0.05	1.37 ± 0.44	0.71 ± 0.10	3.81 ± 1.27
Right aorta	0.19 ± 0.07	0.10 ± 0.04	1.30 ± 0.36	0.70 ± 0.12	3.76 ± 1.30
Left epigastric	0.14 ± 0.04	0.08 ± 0.02	0.86 ± 0.30	0.52 ± 0.11	2.2 ± 0.57
Right epigastric	0.19 ± 0.05	0.11 ± 0.04	1.04 ± 0.41	0.58 ± 0.12	2.6 ± 0.84
Left internal iliac	0.13 ± 0.05	0.08 ± 0.04	0.65 ± 0.45	0.46 ± 0.13	1.95 ± 0.54
Right internal iliac	0.13 ± 0.05	0.08 ± 0.04	0.83 ± 0.61	0.48 ± 0.16	2.16 ± 0.86

Mean ± standard deviation are presented.

(Dangerfield et al., 1976; Cucu, 1977). The absence of physiological parameters could be a principal obstacle to reaching a diagnosis of circulatory failure in this animal group.

The heart rate observed in our study and its negative correlation with body mass agrees with data cited by previous authors for the species (Chittick et al., 2002; Hochscheid et al., 2002). Physical distress due to manual restraint and some room temperature oscillation during examination could be responsible for the beat increase observed in two sub-adult turtles.

The small acoustic window created by the scapular girdle bones, carapace and plastron bones limited access to the aortic arteries and did not allow transducer rotation to obtain different views as is possible in dogs, where the left caudal (apical) parasternal location is commonly used to measure left ventricular outflow tract and aortic root blood flow velocities (Kienle and Thomas, 2002).

The atypical aortic waveform observed in this study seems to reflect the differences in the cardiovascular anatomy and physiology between mammals and reptiles. For example, in sea turtles there are two aortic arteries, the shunted ventricle is partially divided into three chambers (*cavum pulmonare*, *cavum venosum* and *cavum arteriosum*) and the animals have low blood viscosity (Wells and Baldwin, 1994). In sea turtles, the blood flow can be altered to shunt either deoxygenated blood to the lungs or oxygenated blood to the body, providing the animal with greater control over its blood flow, allowing long diving times (Hicks, 2002).

When the lungs are being ventilated and pulmonary resistance is low, as much as 60% of the cardiac output goes to the lungs (Murray, 2006a). In this case, during normal respiration, atrial systole causes blood to flow into the single ventricle filling the *cavum pulmonare* and *venosum*. Concurrently, pulmonary blood runs from the left atrium into the *cavum arteriosum*. During the ventricular systole, blood from the *cavum venosum* and *pulmonare* flows to the low-pressure pulmonary circuit and blood from the *cavum arteriosum* is forced through the partially contracted *cavum venosum* to exit the heart via the left and right aortic arches (Murray, 2006a).

According to one hypothetical analysis illustrated by Hicks (2002), in this kind of circulation, the ratio of peak systolic blood pressure in the systemic and pulmonary flows is close to 1:1. The heart functions as a single pressure

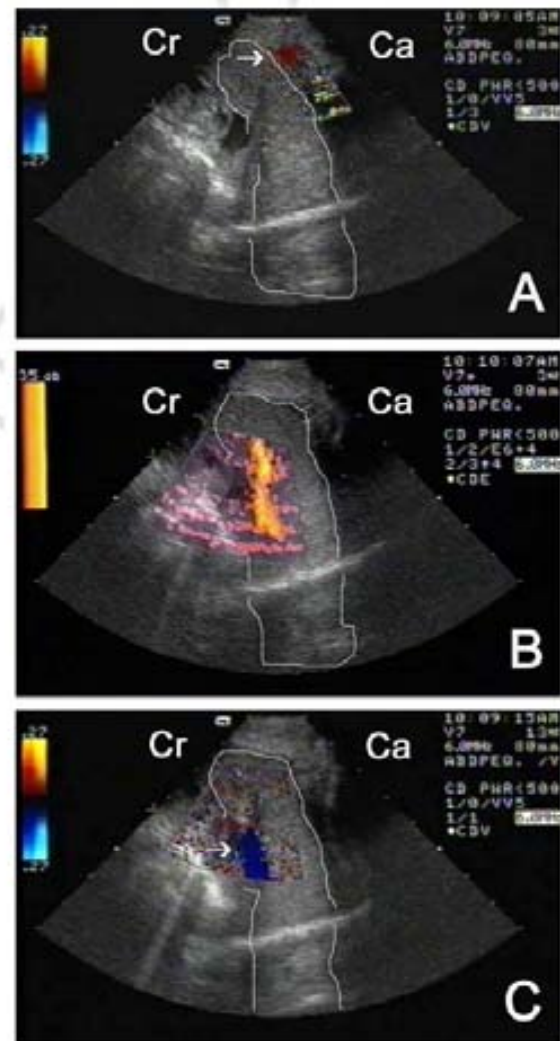


Fig. 4. Ultrasound colour Doppler view of loggerhead sea turtle kidney. (A) Arrow indicates the left epigastric artery. (B) Presence of blood flow (seen in yellow, energy Doppler amplitude flow) in the cranio-ventral part of the kidney. (C) Renal vein. Cr, cranial; Ca, caudal. (For interpretation of the references to colour in this figure legend, the reader is referred to the web version of this article.)

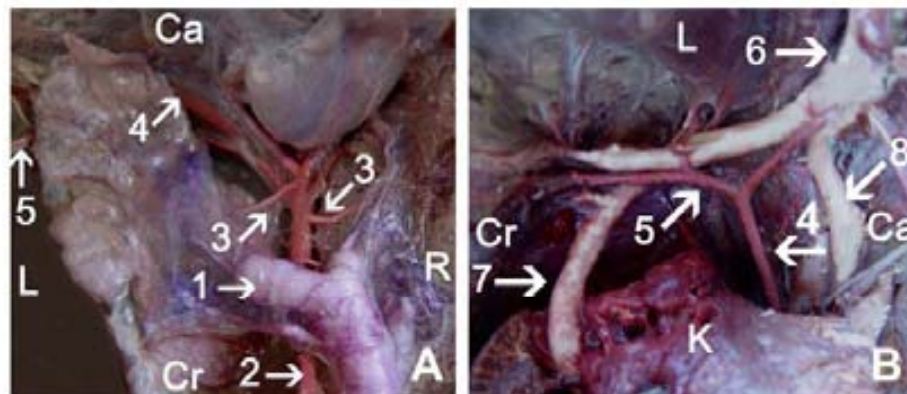


Fig. 5. Gross anatomical dissection of a loggerhead sea turtle kidney. (A) Ventral view. (B) Dorso-lateral view (kidney partially removed). K, dorsal face of kidney; 1, renal vein; 2, abdominal aorta artery; 3, renal arteries; 4, external iliac artery; 5, epigastric artery; 6, iliac vein; 7, epigastric vein (lateral renal portal vein); 8, hypogastric vein (caudal renal portal vein).



Fig. 6. Ultrasound view through postfemoral acoustic window of a loggerhead sea turtle. 1, internal iliac artery; 2, ilium.

pump, with shunt direction and magnitude varying by changes in pulmonary and systemic vascular resistances. The mammalian ratio of systemic to pulmonary vascular resistance is between 7.0 and 10.0 (Van den Bos et al., 1982). Since differences in flow wave shapes can be explained by the amount of reflection in the vascular bed (Van den Bos et al., 1982), the phylogenetic development of a double circulation with systemic and pulmonary vascular circuits (high-pressure and low-pressure circulations, respectively) in mammals could be the principal cause of the differences found in the aortic profiles, PI and RI of the loggerhead sea turtle compared with dogs (Miño et al., 2004).

Ventricular contraction tends to bring the heart apex to the muscular ridge separating the *cavum pulmonare* from the *cavum arteriosum* and *venosum*, thereby creating a barrier against the flow of blood from the *cavum arteriosum* into the *cavum pulmonare*. The exaggerated (hyperdynamic) ventricular wall motion observed in our study is considered normal for chelonians (Murray, 2006a) and is also present in dogs with left-to-right shunts or valvular

regurgitation when end-diastolic volume is increased and end-systolic volume is normal to slightly increased (Kienle and Thomas, 2002).

The hepatic flow velocity waveform found in our study resembles those known for the dog and the ball python with A, C and V-waves being identified (Finn-Bodner and Hudson, 1998; Starck and Wimmer, 2005). However, unlike those findings, the spectrum was observed above the baseline in our study. Interpretation of the flow direction is related to transducer positioning and anatomical features of the species examined. In dogs, ultrasonographic examination of the hepatic vein is performed by placing the transducer on the ventral midline directly caudal to the xiphoid process of the sternum, with caudal-cranial orientation of the ultrasound beam (Mattoon et al., 2002). In the ball python, the images were obtained by placing the transducer on the left side of the large ventral scales, with the caudal part of the gallbladder being used as a landmark (Starck and Wimmer, 2005). In both species the ultrasound beam crosses the liver caudo-cranially, in the same direction as the blood flow in the hepatic veins. A positive Doppler shift is obtained if the beam is aligned in the direction of the flow whereas a negative signal (below the baseline) is present when the flow is away from the beam (Nicolaidis et al., 2002). In the loggerhead sea turtle the right hepatic vein was assessed at its most cranial point, through the axillary acoustic window, therefore the flow was observed coming up to the transducer which could explain the above baseline pattern observed.

Another difference with the dog is the A and C-wave flow velocity. The A-wave represents the blood flow velocity in the hepatic vein during atrial diastole and the C-wave represents the blood flow velocity in the vein during the ventricular diastole (Pozniak, 2002). Flow velocity peak in the C-wave was higher than that in the A-wave in the loggerhead sea turtle in the present study. This pattern has also been observed in ball pythons (Starck and Wimmer, 2005) and

could be related to the hyperkinetic motion of the ventricle during ventricular diastole when the ventricle presses against the filled atria at the same time as the atrioventricular monocusp valve is opened, causing a more rapid expulsion of the blood from the atria. Additionally, the right atrium fills two of the three compartments of the single ventricle, the *cavum venosum* and *cavum pulmonale*, while blood from the left atrium passes directly to the *cavum arteriosum* (Murray, 2006a). During the atrial systole the flow nearly stops and a slight reverse flow was observed, as occurs in dogs (Finn-Bodner and Hudson, 1998).

There is a great paucity of interpretative studies of the Doppler spectrum in reptiles. The low resistance flow pattern observed in the arteries studied here, indicated by broad systolic peaks and continuous, high velocity flow in diastole with gradually decreasing velocity (Pozniak, 2002), has also been seen in the ball python in a postprandial condition (Starck and Wimmer, 2005) and suggests that the loggerhead sea turtle's organs need a continuous blood supply. Normal peak flow velocities in systole in the outflow tract regions and proximal large vessels in dogs and cats are usually around 1 m/s with some patients having velocities approaching 2 m/s (Kienle and Thomas, 2002). In sea turtles we found flow velocities 10 times less than those described. The pulsatility (PI) and resistive (RI) indices in the aortic arteries were lower than those described for dogs, where PI and RI in the abdominal aorta artery were 3.09 and 0.91, respectively (Miño et al., 2004). PI and RI values from other reptilian species were not found in the literature.

Anatomical studies on the renal portal system have been carried out in various chelonian species, and anatomical terminology applied to the vessels has been confusing. Wyneken (2001) stated that in sea turtles the hypogastric vein enters the kidneys posteriorly and ventrally. The renal portal veins drain from the dorsal kidney capillaries into the external iliacs at the level of the epigastric veins, or into the posterior extent of the abdominal vein. However, in this work the schematic drawing presented does not permit clear identification of the hypogastric vein. Other authors (Holz et al., 1997; Holz, 2006) have described the afferent renal portal veins in the red-eared slider as being the iliac and hypogastric veins or generically renal portal veins.

We have assumed that the hypogastric vein is a branch of the external iliac vein referred to as the circumflex iliac vein by Holz et al. (1997). The iliac vein described by these authors as entering approximately two-thirds of the way caudal to the cranial pole of the kidney is the same as that observed in the anatomical dissections of turtles in the current study which been termed the epigastric vein. These important renal veins could not be visualised and measured in the ultrasonographic examination due to the small acoustic windows. For example, the epigastric vein runs close to the carapace bone along its lateral curvature, passing just dorsal to the prefemoral fossa, in an area inaccessible to the ultrasound beam.

To measure heart rate in chelonians, Murray (2006b) indicated the usefulness of the Doppler flow detector

placed directly over the carotid artery. In sea turtles this artery would seem not to be as accessible as in others species of chelonians because of its deep position and the large muscular neck. The internal iliac arteries could therefore be used as an alternative way to check the heart rate in large turtles, when access to the carotid and aortic arches, either through the neck or cervicobrachial acoustic windows, is difficult.

Conclusion

The Doppler waveform of the aortic arteries of loggerhead sea turtle differs from that known in mammals in that the plug flow pattern and the clear spectral window are not consistently observed. The low resistance flow pattern found in these large arteries reflects peculiarities in the cardiovascular anatomy and physiology of the reptiles, such as the presence of two aortas and the shunted ventricle. Consequently, peak systolic velocity, mean velocity, pulsatility and resistive indices of the both right and left aortic arteries of the loggerhead sea turtle are smaller than those recorded for the abdominal aorta of the dog. The hepatic vein flow velocity waveform of the loggerhead sea turtle is similar to that of the dog, although the flow velocity of the C-wave is higher than that of the A-wave. The vessels (hypogastric and epigastric veins) that form the renal portal system in the loggerhead sea turtle are similar to those found in the red-eared slider, although with differing nomenclature used by previous authors.

Based on the results of this study, we conclude that Doppler ultrasonography could be an important tool in detecting quantitative changes in blood flow in the loggerhead sea turtle. Normal patterns and flow values provided in this study could help in the future assessment or evaluation of cardiovascular disorders in injured turtles. Additional studies using similar Doppler parameters including an increased number of turtles and adult individuals are needed in order to complement the database on loggerhead sea turtle blood flow.

Acknowledgements

The authors would like to thank DVM Rosa Novellas DVM Encarna Casas Díaz and DVM Gregorio Mentaberre García for their help in this work.

References

- Balazs, G.H., 1986. Resuscitation of a comatose green turtle. *Herpetological Review* 17, 79–80.
- Chittick, E.J., Stamper, M.A., Bensley, J.F., Lewbart, G.A., Horne, W.A., 2002. Medetomidine, ketamine, and sevoflurane for anesthesia of injured loggerhead sea turtles: 13 cases (1996–2000). *Journal of the American Veterinary Medical Association* 221, 1019–1025.
- Fernández del Palacio, M.J., Fuentes, V.L., Bonagura, J.D., Schober, K.E., Hatfield, D.G., Laughlin, M.H., 2003. Evaluation of transcutaneous Doppler ultrasonography for measurement of blood flow in the femoral artery of pigs. *American Journal of Veterinary Research* 64, 43–50.

- Finn-Bodner, S.T., Hudson, J.A., 1998. Abdominal vascular sonography. *Veterinary Clinics of North America: Small Animal Practice* 26, 887–942.
- Glagov, S., Zarins, C., Giddens, D.P., Ku, D.N., 1988. Hemodynamics and atherosclerosis. Insights and perspectives gained from studies of human arteries. *Archives of Pathology and Laboratory Medicine* 112, 1018–1031.
- Hicks, J.W., 2002. The physiological and evolutionary significance of cardiovascular shunting patterns in reptiles. *News in Physiological Science* 17, 241–245.
- Hochscheid, S., Bentivegna, F., Spaulma, J.R., 2002. Regional blood flow in sea turtles: implications for heat exchange in an aquatic ectotherm. *Physiological and Biochemical Zoology* 75, 66–76.
- Holz, P., 2006. Renal anatomy and physiology. In: Mader, D.R. (Ed.), *Reptile Medicine and Surgery*. Elsevier Inc., Philadelphia, pp. 135–144.
- Holz, P., Barker, I.K., Crawshaw, G.J., Dobson, H., 1997. The anatomy and perfusion of the renal portal system in the red-eared slider (*Trachemys scripta elegans*). *Journal of Zoo and Wildlife Medicine* 28, 378–385.
- Kagawa, Y., Hirayama, K., Uchida, E., Izumisawa, Y., Yamaguchi, M., Kotani, T., Niiyama, M., Yoshino, T., Taniyama, H., 1998. Systemic atherosclerosis in dogs: histopathological and immunohistochemical studies of atherosclerotic lesions. *Journal of Comparative Pathology* 118, 195–206.
- Kienle, R.D., Thomas, W.P., 2002. Echocardiography. In: Nyland, T.G., Mattoon, J.S. (Eds.), *Small Animal Diagnostic Ultrasound*. W.B. Saunders Co., Philadelphia, pp. 354–423.
- Mattoon, J.S., Auld, D.M., Nyland, T.G., 2002. Abdominal ultrasound scanning techniques. In: Nyland, T.G., Mattoon, J.S. (Eds.), *Small Animal Diagnostic Ultrasound*. W.B. Saunders Co., Philadelphia, pp. 49–81.
- Miño, N., Espino, L., Suárez, M., Santamarina, G., Barrero, A., 2004. Estudio de la aorta abdominal mediante Doppler spectral pulsado en perros. *Archivos de Medicina Veterinaria* 36, 87–92.
- Murray, M.J., 2006a. Cardiopulmonary anatomy and physiology. In: Mader, D.R. (Ed.), *Reptile Medicine and Surgery*. Elsevier Inc., Philadelphia, pp. 124–134.
- Murray, M.J., 2006b. Cardiology. In: Mader, D.R. (Ed.), *Reptile Medicine and Surgery*. Elsevier Inc., Philadelphia, pp. 181–195.
- Nicolasides, K., Rizzo, G., Hecker, K., Ximenes, R., 2002. Doppler in Obstetrics. Basic Principles. www.centrus.com.br (Consulted in December 1, 2006).
- Pozniak, M.A., 2002. Ecografía Doppler del hígado. In: Allan, P.L., Dubbins, P.A., Pozniak, M.A., McDicken, W.N. (Eds.), *Ecografía Doppler clínica*. Ediciones Harcourt S.A., Madrid, pp. 123–168.
- Rostal, D.C., Robeck, T.R., Owens, D.W., Kramer, D.C., 1990. Ultrasound imaging of ovaries and eggs in Kemp's Ridley sea turtles (*Lepidochelys kempi*). *Journal of Zoo and Wildlife Medicine* 21, 27–35.
- Stabenau, E.K., Moon, P.F., Heming, T.A., 2001. Resuscitation of sea turtles. *Marine Turtle Newsletter* 62, 3–5.
- Starck, J.M., Wimmer, C., 2005. Patterns of blood flow during the postprandial response in ball pythons, *Python regius*. *The Journal of Experimental Biology* 208, 881–889.
- Szatmári, V., Sótónyi, P., Vörös, K., 2001. Normal duplex Doppler waveforms of major abdominal blood vessels in dogs: a review. *Veterinary Radiology & Ultrasound* 42, 93–107.
- Valente, A.L., Pargá M.L., Espada, Y., Lavin, S., Alegre, F., Marco, I. and Cuenca, R., in press. Normal ultrasonographic imaging of the loggerhead sea turtle (*Caretta caretta*). *Veterinary Record*.
- Van den Bos, G.C., Westerhof, N., Randall, O.S., 1982. Pulse wave reflection: can it explain the differences between systemic and pulmonary pressure and flow waves? *Circulation Research* 51, 479–485.
- Wells, R.M.G., Baldwin, J., 1994. Oxygen transport in marine green turtle (*Chelonia mydas*) hatchlings: blood viscosity and control of haemoglobin oxygen-affinity. *Journal of Experimental Biology* 188, 103–114.
- Wyneken J., 2001. *The Anatomy of Sea Turtles*. U.S. Department of Commerce NOAA Technical Memorandum NMFS-SEFSC 470, pp. 1–172.